ADVANCES IN ATMOSPHERIC SCIENCES, VOL. 38, JULY 2021, 1101–1114

• **Original Paper** •

Characteristics of Chemical Speciation in PM_1 in Six Representative Regions in China

Kaixu BAI[1,2], Can WU[1], Jianjun LI[3], Ke LI[1], Jianping GUO[4], and Gehui WANG[*1,2]

[1]*Key Laboratory of Geographic Information Science (Ministry of Education), School of Geographic Sciences, East China Normal University, Shanghai* 200241, *China*

[2]*Institute of Eco-Chongming*, 20 *Cuiniao Rd., Chongming, Shanghai* 202162, *China*

[3]*State Key Laboratory of Loess and Quaternary Geology, Institute of Earth Environment, Chinese Academy of Sciences, Xi'an* 710079, *China*

[4]*State Key Laboratory of Severe Weather, Chinese Academy of Meteorological Sciences, Beijing* 100081, *China*

(Received 20 July 2020; revised 28 October 2020; accepted 21 December 2020)

ABSTRACT

A better knowledge of aerosol properties is of great significance for elucidating the complex mechanisms behind frequently occurring haze pollution events. In this study, we examine the temporal and spatial variations in both PM_1 and its major chemical constituents using three-year field measurements that were collected in six representative regions in China between 2012 and 2014. Our results show that both PM_1 and its chemical compositions varied significantly in space and time, with high PM_1 loadings mainly observed in the winter. By comparing chemical constituents between clean and polluted episodes, we find that the elevated PM_1 mass concentration during pollution events should be largely attributable to significant increases in organic matter (OM) and inorganic aerosols like sulfate, nitrate, and ammonium (SNA), indicative of the critical role of primary emissions and secondary aerosols in elevating PM_1 pollution levels. The ratios of $PM_1/PM_{2.5}$ are found to be generally high in Shanghai and Guangzhou, while relatively low ratios are seen in Xi'an and Chengdu, indicating anthropogenic emissions were more likely to accumulate in forms of finer particles. With respect to the relative importance of chemical components and meteorological factors quantified via statistical modeling practices, we find that primary emissions and secondary aerosols were the two leading factors contributing to PM_1 variations, though meteorological factors also played important roles in regulating the dispersion of atmospheric PM.

Key words: PM_1 pollution, chemical speciation, secondary aerosol, field campaign

Citation: Bai, K. X., C. Wu, J. J. Li, K. Li, J. P. Guo, and G. H. Wang, 2021: Characteristics of chemical speciation in PM_1 in six representative regions in China. *Adv. Atmos. Sci.*, **38**(7), 1101−1114, https://doi.org/10.1007/s00376-020-0224-2.

Article Highlights:

- PM_1 and its chemical compositions in China varied significantly in space and time.
- PM_1 loading in China was mainly regulated by primary emissions and secondary aerosols.
- Meteorological conditions played important roles in modulating PM_1 loading in Shanghai.
- PM pollution in Shanghai and Guangzhou were mainly caused by submicron particles.

1. Introduction

Aerosols are a critical component of the Earth's atmosphere and play important roles in deteriorating air quality and changing climate (Xin et al., 2015; Guo et al., 2017; Li et al., 2017, 2019; Lou et al., 2019; Zhao et al., 2020). Due to the light extinction effect, aerosols in the atmosphere can significantly degrade the visibility (Charlson, 1969; Appel et al., 1985; Shi et al., 2014). By scattering and absorbing solar and terrestrial radiation, atmospheric aerosols can significantly alter the Earth's radiation budget, which in turn changes the climate through complex cloud-aerosol-precipitation interactions (Guo et al., 2017; Li et al., 2019; Zhao et al., 2020). Moreover, atmospheric aerosols have negative impacts on human health by causing respiratory and cardiovascular diseases, especially those in the forms of fine particulate matter (Ebenstein et al., 2017; Burnett et al., 2018; Zou et al., 2019; Yue et al., 2020).

Aerosols in the ambient environment commonly exist

* Corresponding author: Gehui WANG
Email: ghwang@geo.ecnu.edu.cn

in the form of atmospheric particulate matter (PM), which is a compound of multiple minerals and materials originating from nature and anthropogenic emissions. Given different compounds, the climatic and environmental effects of aerosols are thus determined by both physical properties (e.g., particle size) and chemical constituents of PM (Pósfai and Buseck, 2010; Yang et al., 2011; Xin et al., 2015; Zhang et al., 2018). It is known that mass concentrations of PM and chemical compositions are determined by many factors including primary emissions, chemical reactions, depositions, as well as meteorological conditions that control both local dispersion and long-range transport of PM (Yang et al., 2011; Wang et al., 2014, 2019). Measuring chemical components in PM is thus crucial for understanding the formation of atmospheric aerosols, especially the complex mechanisms behind frequently occurred haze pollution events (e.g., Wang et al., 2016, 2017, 2020).

Observational networks have been extensively established to monitor the physical, chemical, and optical properties of atmospheric aerosols worldwide, such as the Aerosol Robotic Network (AERONET) (Holben et al., 1998) and Global Atmosphere Watch: Aerosols (GAW) (WMO, 2001). Such networks provide ample observational data to help improve understanding of aerosol properties around the world. Similar networks were also established in China. In 2011, the Chinese Academy of Sciences (CAS) launched the Campaign on Atmospheric Aerosol Research network of China (CARE-China). This is also the first comprehensive research platform for observing atmospheric aerosols in the country, aiming to provide in situ measurements of anthropogenic aerosol emissions to better understand the climatic and environmental effects of aerosols in China (Xin et al., 2015).

By taking advantage of such invaluable in situ measurements, complex atmospheric haze pollution mechanisms in China have been better elucidated (Guo et al., 2014; Huang et al., 2014; Wang et al., 2020). For instance, based on chemical data observed in representative mega cities across China, Yang et al. (2011) found that $PM_{2.5}$ mass concentrations and chemical compositions varied substantially over space and that the observed severe $PM_{2.5}$ pollution events in eastern China were largely attributable to local formation/production and regional transport of the secondary aerosols. Utilizing field measurements of aerosol properties at an urban site in Beijing during January and February 2015, Zamora et al. (2019) found that frequently occurring wintertime haze events in Beijing were attributable to the efficient nucleation and secondary aerosol growth under high gaseous precursor concentrations and stagnant air conditions. Likewise, by taking advantage of comprehensive measurements and modeling simulations, Huang et al. (2020) found that the haze events during the COVID-19 lockdown in eastern China were driven by the formation of substantial secondary aerosols due to increases in atmospheric oxidizing capacity.

Given the adverse effect on public health, $PM_{2.5}$ mass concentration and its speciation have been extensively examined in the literature (Yang et al., 2011; Zamora et al., 2019). In the present study, emphasis is given to even finer aerosols with an aerodynamic size less than 1.0 μm, which is also known as submicron PM (abbreviated as PM_1 hereafter). Given this smaller size, PM_1 has higher extinction efficiency and larger negative health impacts (Shi et al., 2014). Therefore, evaluating the variability of PM_1 and its chemical speciation in space and time is of great significance for understanding of its important roles in haze formation and visibility degradation.

By using three-year-long aerosol measurements that were sampled in six representative cities in China, here we aim to first examine variations in PM_1 and its major chemical compositions in space and time, and then to explore their potential roles in the formation of severe fine particle pollution events. The following science questions are to be answered: (1) What chemical constituents were dominant factors in elevating PM_1 pollution levels in the selected regions? (2) Was there a common mechanism for the formation of PM_1 pollution events across these regions? and (3) Did meteorological conditions play important roles in modulating PM_1 pollution levels?

2. Data and Methods

2.1. *Field campaign and instruments*

In this study, aerosol measurements collected from the CARE-China network at six distinct regions during the period of 2012 to 2014 were used. These six sampling sites were deployed in different geographic regions representative of diverse emission types given different population size and urbanization levels. Table 1 gives a brief description of geographic location and the ambient background (rural or urban site) of these six sampling sites. Among them, the site over Qinghai Lake (abbreviated as QHL hereafter) is referred to as a background site since it was deployed in the Tibetan Plateau where it was less influenced by human activity. In contrast, the other five sites were all deployed in urban regions, thereby representing a pollution regime that was highly influenced by anthropogenic emissions (Ren et al., 2018).

Size-segmented atmospheric PM was collected using nine-stage Anderson samplers (Anderson Series 20–800, United States) at an airflow rate of 28.3 L min^{-1} with cutoff sizes of 9.0, 5.8, 4.7, 3.3, 2.1, 1.1, 0.7 and 0.4 μm. Each set of aerosol samples were measured twice monthly, with every data collection task lasting for three days at five urban sites, while six days were used at the QHL site to guarantee an adequate number of valid samples. More detailed description of sampling collection and storage can be found in the literature like Ren et al. (2018) and Xin et al. (2015).

A DRI 2001 thermal/optical carbon analyzer was used to measure organic carbon (OC) and elemental carbon (EC) compositions in size-resolved particles at each sampling site by following the Interagency Monitoring of Protected

Table 1. Geolocation and ambient background information of six aerosol sampling sites used in this study. The abbreviation of each city/region was shown in brackets.

Region	Longitude (°E)	Latitude (°N)	Location and property of monitoring sites
Qinghai Lake (QHL)	101.32	37.62	At the northwestern rim of Qinghai Lake and referred to as the rural background site
Ürümqi (UMQ)	87.68	43.77	On the rooftop of a 10 m-high building on the campus of the Institute of Desert Meteorology at the urban center
Xi'an (XA)	108.95	34.27	On the rooftop of a 10 m-high building on the campus of the Institute of Earth Environment of CAS at the downtown area
Chengdu (CD)	104.06	30.67	On the rooftop of a 10 m-high building on the campus of Chengdu Institute of Plateau Meteorological at the urban center
Shanghai (SH)	121.48	31.22	On the rooftop of Shaw House on the campus of Fudan University in the city
Guangzhou (GZ)	113.23	23.16	On the rooftop of a 50 m-high building on the campus of the South China Institute of Environmental Science at the urban center

Visual Environments (IMPROVE) thermal/optical reflectance (TOR) protocol (Chow et al., 2004, 2007). Meanwhile, soluble inorganic salts including five cations (Na^+, NH_4^+, K^+, Mg^{2+}, and Ca^{2+}) and three anions (Cl^-, NO_3^-, and SO_4^{2-}) were analyzed by ion chromatography (IC), which was equipped with a separation column and a suppressor (Xin et al., 2015). A detailed descriptions of instrumentation and analytic procedures to measure these compositions can be found in Xin et al. (2015).

In this study, PM with aerodynamic diameter no more than 1.1 μm were aggregated to represent PM_1. Mass concentrations of PM_1 and five major chemical compositions of OC, EC, sulfate (SO_4^{2-}), nitrate (NO_3^-), and ammonium (NH_4^+), were extracted and analyzed. To account for unmeasured atoms, organic mass (OM) was derived by multiplying a commonly suggested scale factor of 1.4 to OC concentration, though this scale is subject to many factors and may vary with seasons (Turpin and Lim, 2001; Bae et al., 2006; Yang et al., 2011).

2.2. *Meteorological data*

Meteorological conditions are believed to play important roles in modulating ambient PM concentrations other than primary emissions since they can modulate the dispersion and accumulation of PM (Zheng et al., 2017; An et al., 2019). Four primary meteorological factors that are highly associated with aerosol variations—air temperature *(T)*, wind speed (WS), relative humidity (RH), and boundary layer height (BLH)—were hereby used. All these data were retrieved from the Meteorological Information Comprehensive Analysis and Process System (MICAPS), except BLH, which was retrieved from the ERA-Interim reanalysis that was provided by the European Centre for Medium-Range Weather Forecasts (ECMWF). 3-h MICAPS data at the sampling sites were averaged for every 24-hour to approximate daily averages.

2.3. *Random forest*

To better understand the haze formation mechanisms over the selected regions, we attempted to resolve statistical associations between PM_1 and chemical species as well as meteorological factors at each individual site. The ultimate goal is to evaluate the relative importance of each factor contributing to PM_1 loading levels to determine the leading influential factors in each city. The random forest (RF) method was hereby used to statistically link PM_1 mass concentration to its five major chemical species and four meteorological factors. The reason to use the random forest method is twofold. First, RF has a good generalization performance. Second, in contrast to many "black-box" models, RF has a unique variable importance estimation capacity (Ho, 1998; Altmann, et al., 2010).

The relative importance is calculated by estimating the response of out-of-bag error to the random permutation of out-of-bag data across each variable. Therefore, the larger the increase in error budget, the more important the variable. Such a metric is thus oftentimes used to assess the prediction power of the given predictor, enabling us to determine whether the given variable should be included in the modeling process or not. This capacity helps us better understand the intrinsic associations between the response variable and various explanatory factors (Bai et al., 2019a, b). For the configuration of RF models, 500 regression trees were used in each random forest model, while each tree was grown on a bootstrap sample with a random subset of predictors selected at each split. In this study, our focus is not on the RF modeling performance given limited samples (as large as of 72 data pairs given two monthly sampling frequency). Rather, we aimed to evaluate the relative importance of each explanatory variable, i.e., the relative contribution of chemical species and meteorological factors in determining PM_1 mass concentration.

3. Results and discussion

3.1. *Major chemical species in PM_1*

Figure 1 presents the temporal evolutions of PM_1 and five major chemical constituents that were sampled at each individual site during the field campaign between 2012 and 2014. As shown, concentrations of PM_1 and its chemical constituents varied significantly in space and time, with the max-

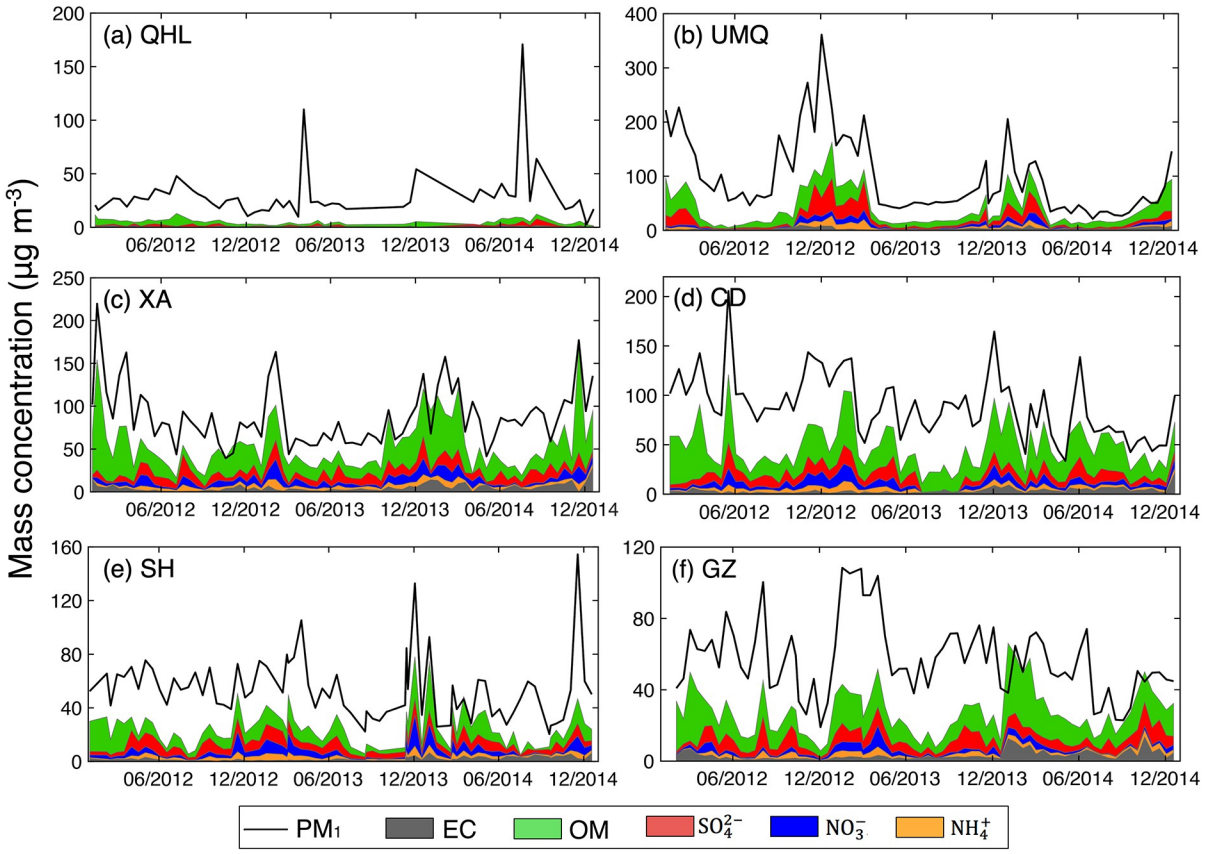

Fig. 1. Temporal evolution of PM_1 mass concentration and five major chemical compositions sampled in six representative cities in China between 2012 and 2014. Note that there were only 53 valid samples measured at the QHL site during the field campaigns.

imum mean PM_1 concentration being triple that of the minimum (29.5–98 μg m^{-3}). Noteworthy is that there were two large outliers (>120 μg m^{-3}) in the PM_1 time series of QHL, and this could be due to possible measurement errors. According to the magnitude of mean PM_1 concentration, these six sampling regions could be generally grouped into three primary pollution regimes as clean (QHL: 29.5±25.1 μg m^{-3}), polluted (SH and GZ: 54.2±23.3 and 57.3±20.9 μg m^{-3}), and severely polluted (XA, CD, and UMQ: 88.1±34.7, 89.7±32.1, and 98±69.5 μg m^{-3}), respectively. Temporally, PM_1 varied even more drastically, as high PM_1 loading (>100 μg m^{-3}) appeared mainly in the winter, whereas low values were seen in the summer. Meanwhile, high PM_1 concentrations were oftentimes accompanied by a substantial increase in chemical constituents such as organic aerosols, sulfates and nitrates, revealing the significance of secondary aerosols in elevating ambient PM_1 loading.

In order to better reveal the spatial and temporal variability of chemical constituents in PM_1 in these six regions, we compared the seasonal mean relative fraction of each chemical species in PM_1. The results are presented in Fig. 2. It is seen that total carbon (OC plus EC) and SNA (the sum of sulfate, nitrate, and ammonium) only accounted for a small portion (<50% in most regions) of PM_1 mass concentration, especially at the QHL site (21.4%). Given low primary emissions around the QHL site due to limited human activity, the low fraction of five major chemical constituents thus implies higher contribution of other components like mineral elements from manmade or natural primary sources to the observed PM_1 mass concentration. However, note-

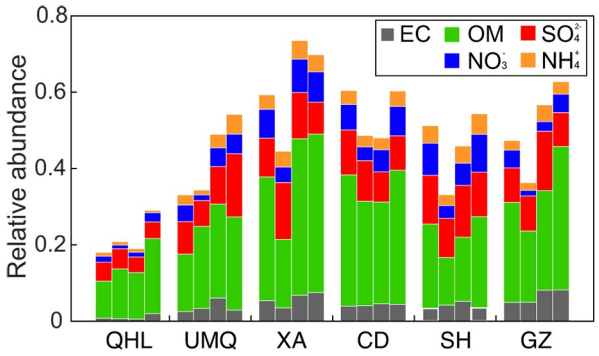

Fig. 2. Seasonal mean relative abundance of five major chemical compositions in PM_1 mass sampled at six representative cities during the 2012–14 field campaigns. Bars from the left to the right for each city indicate the fraction of chemical compositions in spring (MAM), summer (JJA), autumn (SON), and winter (DJF), respectively. Note that only 53 observations were sampled in Qinghai from the field campaigns.

worthy is that the mean PM_1 concentration at the QHL site is even larger than some urban sites around the world, e.g., Vienna (14.9±7.7 μg m^{-3}) (Gomišček et al., 2004). Due to the data availability issue, the element analysis was not performed here to better examine the constituents of PM_1 at the QHL site; hence, reasons for this effect remain unclear.

An inter-comparison between five chemical constituents revealed that OM had the most significant contribution to PM_1 mass concentration since OM alone accounted for a mass fraction as large as of 10%–42% of PM_1 throughout the year at these six sampling sites. Such a high fraction of OM was also found in other cities like Beijing and Tianjin (Shao et al., 2018; Khan et al., 2021). Temporally, this high fraction was even more impressive in the autumn and winter, particularly in cities like Xi'an and Guangzhou where OM increased more drastically during the wintertime than in the summer. This could be attributable to extensive primary emissions from biomass burning and coal combustion in the winter (Li et al., 2014; Wu et al., 2020). In Guangzhou, the increase in OM could be ascribed to both primary and secondary organic aerosols from extensive traffic emissions (e.g., vehicles and ships), since the primary organic pollutants can be easily oxidized to form SOA through gas-phase oxidation chemistry in a wet ambient environment (Yang et al., 2011; Qin et al., 2017).

The SNA only accounted for 7%–23% (a mean value of 17.8%±5.9%) of PM_1 concentration. Notably, sulfate constituted much higher fractions (58%±6.6% of the SNA) than the other two counterparts (25.6%±4.3% for nitrate and 16.4%±3% for ammonium). In contrast, the EC constituted a much lower fraction with a percentage ranging from only 0.9%–6.5%. Spatially, Guangzhou had the largest EC fraction (6.5%) while the smallest fraction (<1%) was observed at the QHL site. Since the field measurements at the QHL were considered as the ambient background values, these inter-comparation results collectively imply that the higher PM_1 mass concentration in the other five major cities could be attributable largely to extensive anthropogenic emissions from primary sources like vehicles and heating related biomass and coal combustion.

Figure 3 compares the seasonal mean mass ratio of OC to EC (OC/EC) and NO_3^- to SO_4^{2-} (NO_3^-/SO_4^{2-}). Noteworthy is that QHL had an extremely large mean OC/EC ratio (22.5) among these six regions, followed by Chengdu (7.4), Ürümqi (6.3), Shanghai (6.0), Xi'an (5.8), and Guangzhou (4.2). Meanwhile, the OC/EC ratio in Guangzhou was found to vary little across seasons, appearing to imply a relatively important role of primary emissions. This could be linked to considerable diesel and low quality bunker fuel powered ships in the Pearl River delta (Yang et al., 2011). On the contrary, the extremely large mean OC/EC ratio at the QHL site was mainly observed during summer and fall periods. Our further investigations showed that OC at the QHL had larger mean concentration (2.6 μg m^{-3}) during summer and fall than in winter and spring (1.9 μg m^{-3}). Given near constant low EC values during the sampling period, we speculate that the observed large OC/EC ratio at the QHL site might be associated with increased OC like biogenic sources (volatile organic compounds) due to higher temperature. Among the five major cities, the largest OC/EC ratio was observed by all in the winter, indicating more significant primary emissions during the wintertime.

The mass ratio of NO_3^-/SO_4^{2-} was also calculated and compared across these six regions. This ratio has been frequently used as an indicator of the relative contribution of mobile sources against stationary sources, with a high mass ratio of NO_3^-/SO_4^{2-} tending to imply a more important role of mobile sources over stationary sources and vice versa (Arimoto et al., 1996; Yao et al., 2002; Yang et al., 2011; Shao et al., 2018). Among these six regions, all annual mean NO_3^-/SO_4^{2-} ratios were lower than 1.0, with the lowest ratio observed at the QHL (0.36), followed by Guangzhou (0.37), Ürümqi (0.41), Shanghai (0.61), Chengdu (0.62), and Xi'an (0.71). Noteworthy is that the NO_3^-/SO_4^{2-} ratio in Guangzhou was the second lowest, which was almost comparable to that of QHL. Given the consensus of larger amounts of vehicles and ships in Guangzhou and Shanghai, the relatively low NO_3^-/SO_4^{2-} ratios in these two cities are thus insufficient to conclude a less important role for mobile sources, since many other contributing factors and even the degree of representativeness of the sampled data were not well accounted for. For instance, the largest

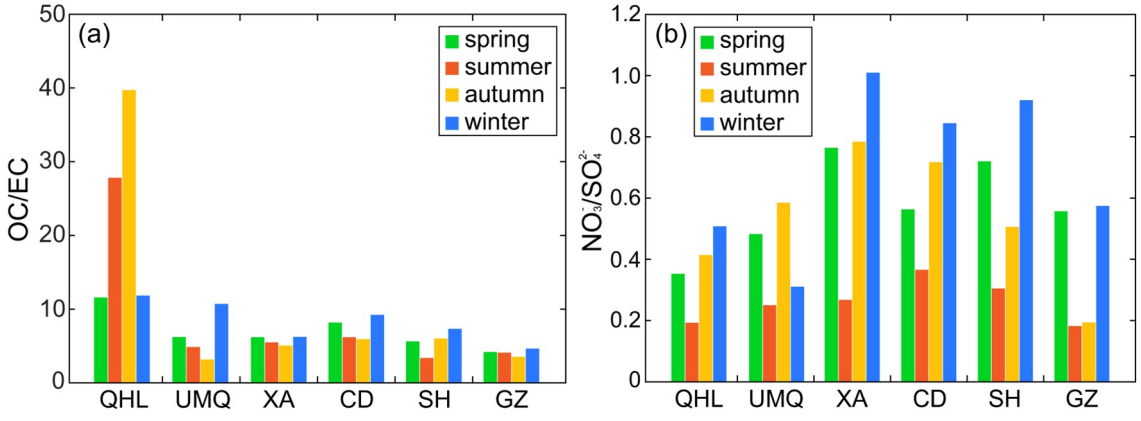

Fig. 3. Same as in Fig. 2 but for seasonal mean mass ratios of (a) OC to EC and (b) NO_3^- to SO_4^{2-}.

NO_3^-/SO_4^{2-} ratios in Xi'an might be more likely associated with extensive coal combustion there (Zhang, 2014), especially in the winter, and thus it could also yield large amounts of wintertime nitrate as well (Wang et al., 2018). Overall, more evidence such as emission inventory should be applied in the future to better examine the relative contribution of mobile and stationary sources to PM_1 pollution levels. Nevertheless, a long-term analysis of NO_3^-/SO_4^{2-} ratio could still be performed in the future to evaluate the shift of the energy consumption structure over the study region (Shao et al., 2018).

The NO_3^-/SO_4^{2-} ratios were also found to exhibit significant seasonal variability, with the largest ratio mainly observed in the winter, except in Ürümqi where the largest ratio emerged in the autumn, while the lowest ratio was observed by all sites in the summer (Fig. 3b). Among these six regions, the largest ratios tripled that of the lowest in cities such as Xi'an, Shanghai, and Guangzhou, particularly in Xi'an where the ratio even exceeded one in the winter. Inter-comparisons of NO_3^-/SO_4^{2-} ratios between summer and winter imply an increased contribution from stationary sources other than mobile sources in the winter, since the latter normally show no significant variation across seasons in urban areas. This could be due to the high vulnerability of volatilization of nitrate salts such as NH_4NO_3 in the summer as well as the fast formation of nitrates under cold and wet weather conditions in the winter (Hu et al., 2011; Liu et al., 2014). On the other hand, nitrate loss could be also a possible factor influencing the NO_3^-/SO_4^{2-} ratios. It is known that quartz exhibits much higher nitrate loss than other filter media such as Teflon and Nylon (Chow et al., 2005), especially for samples from subtropical areas during summer. In other words, the nitrate loss could be uneven between different sampling sites and seasons.

Figure 4 compares the annual cycle of EC, OM, and SNA in PM_1 mass in these six representative regions. Noteworthy is that the sum of EC, OM, and SNA at QHL only accounted for <30% of PM_1 mass throughout the year, except in December and January, when there was a marked increase in OM. Nevertheless, the average ratio was still low (24.7%), even after accounting for other inorganic ions such as K^+, Na^+, Ca^{2+}, Mg^{2+}, Cl^-, and F^-. This implies the spe-

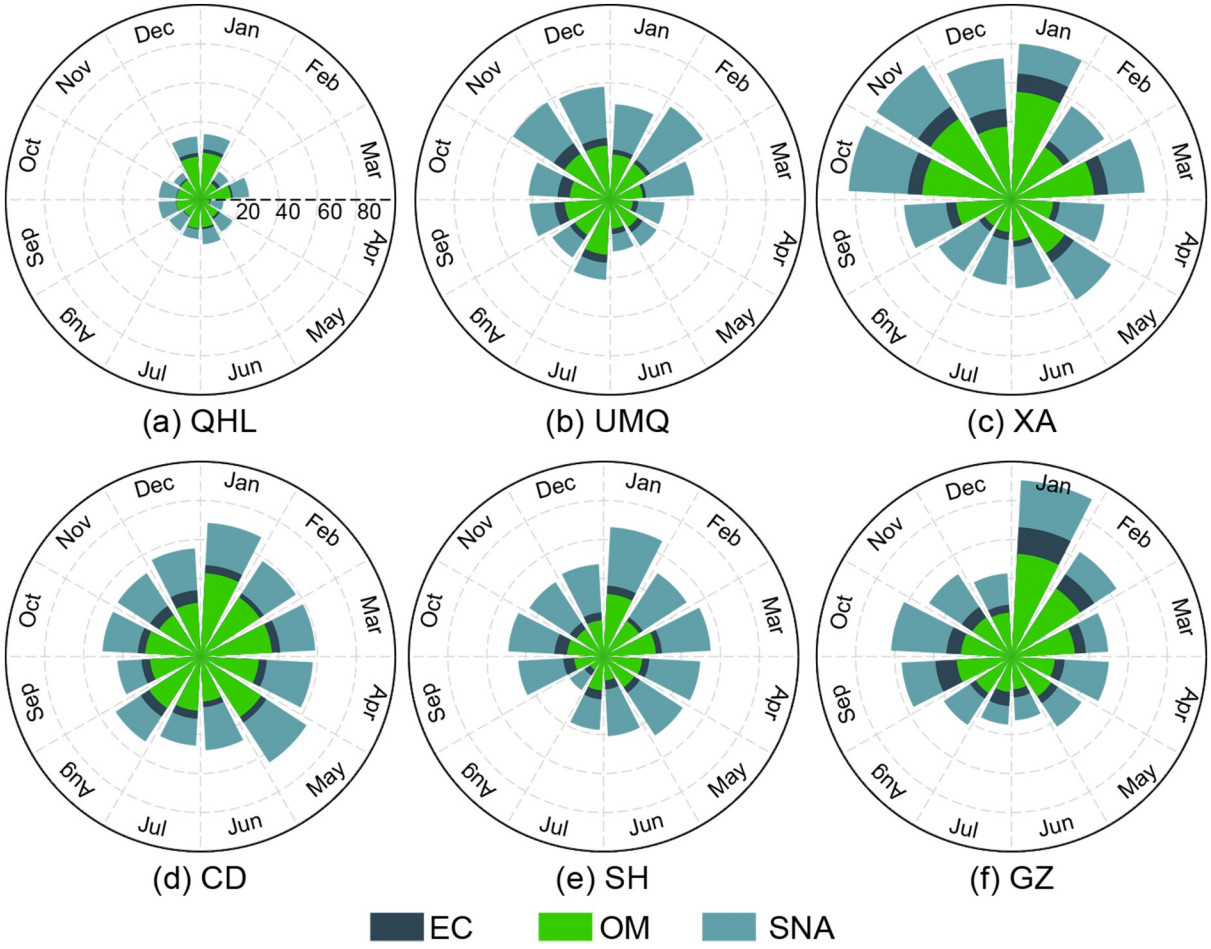

Fig. 4. Monthly mean relative abundance of elemental carbon (EC), organic mass (OM), and secondary inorganic species (denoted as SNA, which is represented by the sum of sulfate, nitrate, and ammonium) in PM_1 mass at six cities across China during 2012–14. A commonly applied factor of 1.4 was applied to convert organic carbon to OM to account for unmeasured atoms in organic species. Note that observations at the QHL station were temporally discontinuous during the field campaigns due to the absence of valid measurements in several months.

cies considered in this study were insufficient to account for PM_1 mass measured at QHL. Conversely, the sum of EC, OM, and SNA constituted more than 80% of PM_1 mass during wintertime in Guangzhou (January) and Xi'an (October, November, and January), especially the latter two components (i.e., OM and SNA), accounting for the vast majority of wintertime PM_1 mass concentration. Overall, the largest fraction was more likely to be observed in January due to a substantial increase in OM and SNA, particularly OM, which increased from about 20% in December to nearly 50% in January in Guangzhou (Fig. 4f). These results clearly revealed significant variations in PM_1 and its speciation in space and time, highlighting the importance of continuous field campaigns, particularly a comprehensive analysis of elements, to better understand the variability of chemical compositions in PM_1 across China.

3.2. *Chemical compositions during clean and polluted days*

To better examine the associations between chemical compositions and PM_1 mass concentrations, particularly their relative roles in elevating PM_1 loading levels, we compared mass concentration of each major chemical composition in PM_1 at each sampling location between distinct pollution episodes. We define clean and polluted episodes according to the relative levels of PM_1 mass concentration in each specific region as days with the smallest and the largest 20% of PM_1, respectively. Detailed comparison results were presented in Table 2.

It is found that PM_1 concentration on polluted days was, on average, 2.6~6.5 times the magnitude of that during clean periods, with the largest increase observed in Ürümqi (6.5), followed by Qinghai (4.6), Shanghai (3.1), Guangzhou (2.8), Chengdu (2.7), and Xi'an (2.7). This also implies PM_1 concentration in Ürümqi experienced the most significant variation over the time covered by the sampling period. On the contrary, PM_1 concentration in Chengdu exhibited a relatively low variability throughout the year. In regard to chemical constituents, the mass concentration of some species during polluted episodes increased by a factor as large as 10 times of that during clean episodes.

During polluted periods, in Qinghai, sulfate almost tripled in concentration compared to that on clean days, while OM, EC, and ammonium doubled their concentrations. In contrast, nitrate maintained a nearly constant concentration. This implies the high PM_1 concentration at QHL was dominated by primary combustion emissions, since emissions from vehicles were negligible around the sampling region. In Ürümqi, there were substantial increases in concentrations of five major chemical compositions as ammonium, nitrate, sulfate, OM, and EC increased by a factor of 11.9, 10.9, 9.5, 4.4, 2.7, respectively. Such a salient increase in these five major compositions inevitably elevated the mass concentration of PM_1. Given the considerable increase in concentrations of SNA, we may largely ascribe the drastic elevation in PM_1 mass concentration during polluted days in Ürümqi to extensive anthropogenic primary emissions. On the other hand, this also could be attributable to enhanced nitrate formation as well as aerosol hygroscopicity due to increased RH during wintertime in Ürümqi resulting from extensive snowfalls, since a similar effect was also observed in north China (Shao et al., 2018; Sun et al., 2020).

Xi'an and Chengdu, two inland mega cities, were found to exhibit similar variations in concentrations of both PM_1 and major chemical compositions. Moreover, their data magnitudes were also comparable. Specifically, PM_1 concentration on polluted days in both cities was 2.7 times of that on clean days. In terms of the five major chemical constituents studied, Xi'an had larger concentrations of EC, OM, nitrate, and ammonium than Chengdu during polluted episodes, especially the former two species as their concentrations in Xi'an significantly exceeded those in Chengdu. These results suggest that primary emissions played a more important role in elevating PM_1 pollution levels in Xi'an, whereas PM_1 pollution in Chengdu could be attributable to larger emissions from stationary sources (e.g., coal combustion) given higher

Table 2. Comparisons of mean mass concentration of PM_1 and chemical compositions (units: μg m^{-3}) during clean and polluted episodes. Here clean and polluted days were defined as days with the lowest and the largest 20% PM_1 mass concentration during the study time period, respectively. *N* denotes the number of samples in each episode and uncertainty of each factor was characterized by plus and minus one standard deviation from the mean value.

Region	Episode	PM_1	EC	OM	NO_3^-	SO_4^{2-}	NH_4^+
Qinghai (*N*=12)	clean	13.96±4.57	0.12±0.10	2.03±1.52	0.33±0.13	0.77±0.53	0.14±0.21
	polluted	59.64±43.40	0.21±0.20	4.03±3.05	0.34±0.22	2.06±1.86	0.33±0.31
Ürümqi (*N*=14)	clean	35.29±6.86	1.74±0.72	9.19±2.17	0.76±0.73	3.14±1.19	0.70±0.48
	polluted	213.76±51.35	4.62±3.47	40.63±14.60	8.26±4.89	29.70±17.08	8.32±5.71
Xi'an (*N*=15)	clean	52.15±7.19	3.20±2.19	18.72±7.74	3.72±2.28	6.85±3.43	2.30±0.99
	polluted	142.29±29.75	7.46±6.75	61.14±29.07	12.47±5.97	12.43±6.50	6.25±3.13
Chengdu (*N*=14)	clean	50.44±8.78	3.11±1.65	17.78±5.23	3.07±1.43	5.34±2.51	1.73±0.79
	polluted	138.41±23.36	3.89±2.00	45.66±14.98	10.32±5.33	12.70±6.33	5.23±2.62
Shanghai (*N*=14)	clean	28.85±4.49	2.05±1.34	5.38±3.63	1.58±1.51	4.40±1.64	1.38±0.71
	polluted	88.33±25.72	2.12±1.70	15.98±8.53	9.79±5.47	9.07±2.50	4.39±1.50
Guangzhou (*N*=14)	clean	30.91±7.55	2.54±2.07	9.23±6.28	0.73±0.38	3.10±1.20	0.70±0.35
	polluted	87.34±14.81	2.93±1.63	17.73±7.16	3.53±2.81	7.72±3.56	2.64±1.21

sulfate loading.

The two mega cites in the coastal regions, Shanghai and Guangzhou, were both found to suffer from similar PM_1 pollution levels given comparable mean PM_1 concentration. It is indicative that PM_1 concentration during polluted days almost tripled that on clean days in both cities. During polluted episodes, concentration of all species except EC was observed to increase significantly in both cities. Noteworthy is that all the remaining four major species were found to increase even more markedly in Shanghai, especially OM (+10.6 μg m^{-3}) and nitrate (+8.2 μg m^{-3}). This implies more important roles of mobile sources in elevating PM_1 pollution levels in Shanghai during haze days. Similar results have also been revealed in the literature (e.g., Shi et al., 2014; Qiao et al., 2016).

Compared to the other four species, EC constituted a relatively low fraction in urban areas. Also, the absolute concentration exhibited small variation between two regimes. This indicates that the phenomenal increase in PM_1 concentration during polluted days should be attributable more to other species such as OM, nitrate and sulfate as their concentrations were found to increase drastically. This finding also corroborates the critical role of the fast formation of secondary aerosols via aqueous reaction in exacerbating regional fine particle pollution levels during polluted periods (Wang et al., 2017, 2019; Yao et al., 2018; Dang and Liao, 2019).

In light of the increases in mean concentrations of PM_1 and five major chemical species, we find that mean PM_1 concentration had increased by 45~178 μg m^{-3} during polluted periods compared to that on clean days (Table 2). However, the accumulated increases in concentration of the five major chemical constituents only accounted for a small fraction of the total increased PM_1 concentration. This implies that the observed high PM_1 loading also should be attributable to factors other than these five major chemical constituents. In other words, it is challenging to resolve PM_1 pollution mechanisms simply based on these five chemical species since they only accounted for a small fraction of the observed increase in PM_1 concentration.

Since severe haze pollution events are oftentimes observed in the winter, we further compared mass concentrations of PM_1 and five major chemical constituents during polluted days in winter and other seasons. As shown in Table 3, higher mean PM_1 concentration was observed during wintertime in Xi'an, Shanghai, and Guangzhou. In Ürümqi, there was a noticeable increase in concentration of OM, sulfate, and ammonium in the winter, especially OM (+12.61 μg m^{-3}) as the mean wintertime concentration was 1.5 times of that in other seasons. This implies more extensive primary emissions in Ürümqi in the winter and that the elevated OM could be attributable to wetter weather due to extensive wintertime snowfalls that boost the formation of SOA.

In Xi'an, all five major chemical compositions were found to have larger mass concentration during the wintertime except OM, especially EC (+4.01 μg m^{-3}), implying the wintertime PM_1 pollution in Xi'an could be ascribed to more extensive primary emissions. In contrast, both PM_1 and the five major chemical constituents were observed to have higher concentration in Chengdu during the wintertime, with the most significant increase found in OM (+12.31 μg m^{-3}), followed by nitrate (+5.45 μg m^{-3}), ammonium (+1.53 μg m^{-3}) and EC (+1.36 μg m^{-3}). This could be due to the enhanced formation of secondary aerosols during the wintertime. In contrast, little difference was observed in chemical compositions between seasons in Guangzhou. Noteworthy is that there was a ubiquitous increase in ammonium during wintertime in these five major cities, though the magnitude was relatively small. These diverse results clearly highlight the complexity behind the formation mechanism of PM_1 pollution events as factors like the formation of SOA and aerosol hygroscopicity could all result in a significant increase in PM_1 loading in the atmosphere (Khan et al., 2021).

3.3. *Impact of meteorological conditions on PM_1 pollution*

In addition to chemical speciation, PM_1 mass concentration was modulated by meteorological conditions, which are believed to play an important role in governing the disper-

Table 3. Same as in Table 2 but for comparisons of mean mass concentration of PM_1 and chemical compositions (units: μg m^{-3}) during polluted days in winter and other seasons. Note that there is only one valid sample in Qinghai during the winter.

Region	Season	*N*	PM_1	EC	OM	NO_3^-	SO_4^{2-}	NH_4^+
Qinghai	winter	1	54.26	0.10	5.20	0.01	0.05	0.01
	others	10	60.18±45.71	0.22±0.20	3.91±3.19	0.37±0.20	2.26±1.83	0.36±0.31
Ürümqi	winter	10	209.51±59.02	3.76±3.50	44.47±13.91	7.31±3.82	29.88±11.81	8.43±4.82
	others	5	210.86±35.85	5.68±3.31	31.86±11.47	10.47±6.07	28.23±25.28	8.33±7.34
Xi'an	winter	9	144.95±32.61	9.10±7.92	59.46±27.59	12.69±6.18	13.00±7.64	6.87±3.27
	others	6	138.30±27.30	4.99±3.88	63.65±33.70	12.13±6.20	11.57±4.83	5.32±2.92
Chengdu	winter	7	132.99±16.78	3.30±2.60	41.96±16.02	12.23±5.20	12.40±4.98	6.16±2.83
	others	8	139.46±29.44	4.05±1.54	45.47±17.04	8.43±4.72	12.63±7.35	4.30±2.05
Shanghai	winter	4	92.98±28.21	3.11±2.76	24.57±11.27	13.35±7.38	9.80±2.67	5.45±1.78
	others	9	84.90±25.22	1.75±0.97	12.26±3.99	7.90±4.21	8.98±2.48	3.92±1.18
Guangzhou	winter	4	99.14±16.10	2.17±0.28	18.40±4.45	4.82±0.43	7.59±2.37	3.13±0.84
	others	10	84.19±12.41	3.30±1.90	18.29±8.05	3.22±3.30	7.98±4.17	2.58±1.32

sion of atmospheric particles and its gaseous precursors. Figure 5 shows the correlation between PM_1 mass concentration and the four meteorological factors of air temperature, wind speed, RH, and BLH, respectively.

Negative correlations were observed between PM_1 mass concentration and air temperature (except at the QHL where exhibited a positive correlation), especially in Ürümqi, Xi'an, and Shanghai, where negative correlations were even statistically significant at the 95% confidence interval. High PM_1 concentrations were mainly observed during cold days, whereas low values were prevalent on hot days. This effect was even more pronounced at Ürümqi and Xi'an, in large part possibly due to the wintertime heating-related extensive coal combustion in these two cities. In addition, stagnant weather was more likely to occur in the winter, which can also elevate PM_1 loading (Shao et al., 2018). For regions like Guangzhou, temperature appeared to have no significant association with PM_1 concentration. This is because temperature is normally high in Guangzhou throughout the year and there is almost no extensive wintertime heating related coal combustion there.

Wind speed exhibited a negative correlation with PM_1 mass concentration in the five major cities (Fig. 5b), which is also in line with our expectation, since wind modulates the diffusion and transport of regional air pollutants. Nevertheless, significant correlations were found only in Ürümqi and Chengdu, indicating wind played critical roles in modulating regional PM_1 concentration levels in these two cities.

Humidity is also a critical factor since it determines the nucleation and hygroscopic growth of particles through gas-liquid reaction process, especially the aqueous-phase oxidation of SO_2 (Wang et al., 2016, 2020; Li et al., 2017; Zheng et al., 2017; Sun et al., 2020). Given the complex process of gas-liquid reaction, the relationship between humidity and PM_1 mass concentration is oftentimes nonlinear and nonstationary, making it challenging to characterize the statistical associations between them. A statistically significant positive correlation was found between RH and PM_1 in Ürümqi, with high pollution levels being more likely to be observed under wetter conditions with RH > 70% (Fig. 5c). A recent study also revealed distinct responses of primary and secondary species in PM_1 and $PM_{2.5}$ to RH due to changes in aerosol hygroscopicity and phase states (Sun et al., 2020).

BLH is another key factor modulating the dispersion and accumulation of air pollutants in the troposphere in addition to wind speed (Guo et al., 2019; Lou et al., 2019), since a low planetary boundary layer can suppress the vertical and

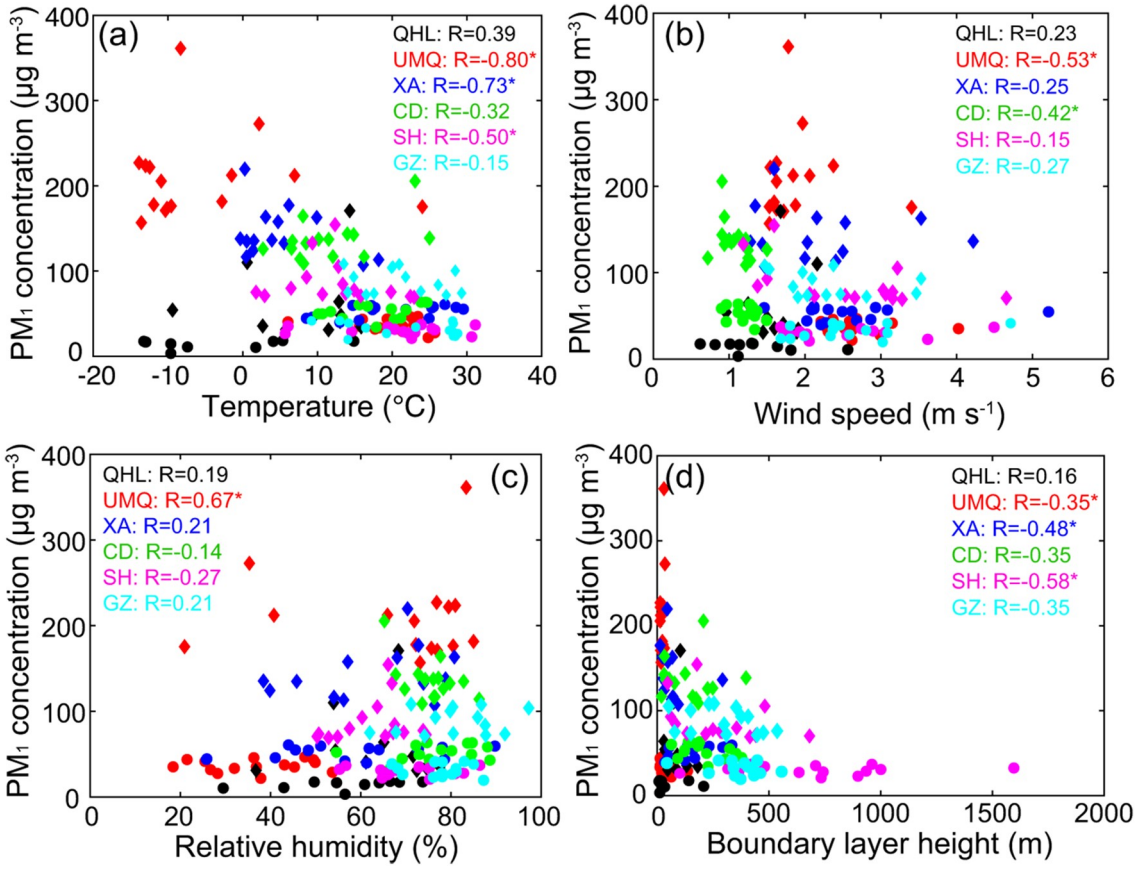

Fig. 5. Correlation between PM_1 mass concentration and four meteorological factors in six representative regions across China. Only data values during clean (circle) and polluted (diamond) days were extracted for the calculation of correlation coefficient. Correlation values marked by asterisk indicate the correlation is statistically significant at the 95% confidence interval.

horizontal diffusion of aerosol, in turn exacerbating the haze pollution (Liu et al., 2018; Miao et al., 2018; Zhu et al., 2018; Bai et al., 2019a). Negative correlations were found between BLH and PM_1 mass concentration in five major cities, with statistically significant correlations (95% confidence interval) observed in Ürümqi (R = –0.35), Xi'an (R = –0.48), and Shanghai (R = –0.58), respectively. It is understood that severe haze pollution events oftentimes are accompanied by a low BLH (<200 m), causing both fine particles and precursors to be suppressed in the lower troposphere near the ground, and accelerating the accumulation of air pollutants and higher PM_1 loading in turn.

Table 4 compares the seasonal mean meteorological conditions during polluted days between winter and other seasons. The results indicate that there were significant yet heterogeneous differences in meteorological conditions between distinct seasons. Generally, the synoptic weather in the winter was oftentimes cold, calm (lower wind speed), along with a low BLH, and even wetter in some regions (e.g., Ürümqi, Chengdu, and Shanghai). Evidently, such a weather condition is favorable to the accumulation of air pollutants (low wind speed and BLH) and the formation of secondary aerosols (cold and wet) (Li et al., 2017; Wang et al., 2017; An et al., 2019). Noteworthy is that synoptic weather appears to have little effect on PM_1 pollution levels in Chengdu despite the similarity in PM_1 concentration and meteorological conditions (except temperature) across seasons. This could be attributable to the basin topography of Chengdu, where air pollutants cannot be easily diluted under a relatively calm weather regime, thereby yielding a near constant ambient PM_1 loading therein.

Figure 6 compares the relative importance of each factor in predicting PM_1 concentration levels at each individual sampling site. As shown, leading factors (i.e., factors with larger relative importance) differed across study regions. Specifically, EC was the leading factor in predicting PM_1 mass concentration at the QHL, implying the variability of PM_1 concentration was highly associated with the loading of EC. Since this region was deemed as the ambient background given limited human activity, it is reasonable to conclude that PM_1 loading in this region is largely modulated by EC from primary emissions occurring there. In Ürümqi, EC and OC were found to play more important roles, indicative of larger contribution of primary sources to PM_1 variations in this region.

In Xi'an, OC played the predominant role compared to other factors, followed by RH, EC, and nitrate. This is indicative of the significant role of secondary aerosols in modulating PM_1 mass concentration there. In contrast, OC and SNA played comparable roles in Chengdu, followed by wind speed. Among them, sulfate had a larger importance than the others, implying more important roles played by stationary sources. Moreover, wind was also a key factor in modulating the dispersion of PM, since air pollutants cannot be easily diluted in Chengdu due to the basin topography. In Shanghai, OC and wind speed were two leading factors, followed by BLH, indicating the critical role of secondary aerosols and meteorological conditions like temperature inversion in modulating PM_1 concentration in this region.

In spite of the low abundance of ammonium and nitrate as compared to other three species, these two species were found to play the most critical roles in modulating the variations in PM_1 mass concentration in Guangzhou (Fig. 6f). Conversely, RH was found to play the least important role, because Guangzhou is located in Pear River estuary, which has a humid subtropical climate, thereby the humidity is high year round. In other words, humidity would not be a key factor limiting the formation of secondary aerosols in a humid region. Ammonium was found to play the most critical role in modulating the variations in PM_1 mass concentration, followed by nitrate. This could be related to the neutralization of NO_3^- by NH_4^+ since NO_3^-, SO_4^-, and NH_4^+ display positive feedback interactions among these constituents, resulting in elevated PM_1 concentration in turn (Shao et al., 2018). The second leading role of nitrate further corroborates the critical role of mobile sources in contributing to PM_1 pollution levels in Guangzhou, which is also in line with previous findings (Yang et al., 2011). These results clearly indicate the relatively important role of secondary aerosols in modulating PM_1 loading variability in Guangzhou.

Table 4. Same as in Table 3 but for meteorological conditions. Note that there is only one valid sample in Qinghai during the winter.

Region	Season	N	T (°C)	WS (m s^{-1})	RH (%)	BLH (m)
Qinghai	winter	1	–9.39	0.96	54.39	34.12
	others	10	9.97±6.07	1.68±0.59	64.60±23.67	89.00±51.85
Ürümqi	winter	10	–11.40±1.84	1.72±0.26	77.09±3.95	20.19±7.60
	others	5	5.78±10.88	2.18±0.71	49.57±25.62	22.96±7.15
Xi'an	winter	9	1.46±1.64	1.89±0.81	58.13±24.97	66.16±78.29
	others	6	9.98±5.94	2.40±1.22	70.17±7.36	95.47±100.10
Chengdu	winter	7	7.25±2.34	1.13±0.20	76.84±4.25	124.74±91.37
	others	8	15.55±5.85	1.05±0.20	74.51±6.40	143.80±124.95
Shanghai	winter	4	5.65±3.84	2.10±0.90	64.95±3.20	209.68±190.34
	others	9	15.04±4.99	2.74±0.93	61.93±9.06	319.77±176.29
Guangzhou	winter	4	17.16±3.89	1.95±0.54	75.06±10.82	154.09±103.69
	others	10	22.56±5.21	2.35±0.69	82.92±8.82	350.48±128.09

3.4. *Ratios of PM_1 to $PM_{2.5}$*

To better understand PM pollution in these six regions, we also compared the mass concentration of PM and five major chemical compositions between PM_1 and $PM_{2.5}$ (using $PM_{2.1}$ as a proxy). Given the simultaneous sampling, we calculated their mass concentration ratios ($PM_1/PM_{2.5}$) and the results are summarized in Table 5. It is seen that PM_1 accounted for 66%–75% mass concentration of $PM_{2.5}$ that were measured in these six regions, which is slightly higher than that in Tianjin (63%) as discovered in Khan et al. (2021). Such a high $PM_1/PM_{2.5}$ ratio implies $PM_{2.5}$ in these six regions was largely dominated by small size particles due to combustion processes and secondary aerosols rather than natural sources and mechanical processes (Khan et al., 2021). Meanwhile, this also highlights the notorious negative health impacts of $PM_{2.5}$ since nearly 70% of its composition is from submicron particles.

Spatially, PM_1 accounted for a larger fraction of $PM_{2.5}$ mass concentration in the two coastal megacities of Shanghai (0.73) and Guangzhou (0.75), where primary emissions from vehicles and ships are normally more extensive than in the two inland megacities of Xi'an (0.66) and Chengdu (0.69). Such a spatial distribution of $PM_1/PM_{2.5}$ ratio is also in line with previous studies in Chen et al. (2018) as high ratios were mainly observed in Southeastern and Central China while low ratios were found in Western China where natural sources are also important contributions. Moreover, this ratio varied with pollution regimes and humidity. For instance, Qiao et al. (2016) found a relatively high $PM_1/PM_{2.5}$ ratio on clean days whereas an elevated ratio of $PM_{1-2.5}/PM_{2.5}$ on hazy days. Sun et al. (2020) also revealed that the changes in $PM_1/PM_{2.5}$ ratios as a function of RH were largely different for primary and secondary aerosol species due to distinct aerosol hygroscopicity and phase states.

In regard to the five major chemical compositions, we found that most major $PM_{2.5}$ constituents in Guangzhou were PM_1 given higher ratios of chemical species, except nitrate and ammonium, which had the largest fraction in Ürümqi (0.72) and Qinghai (0.94), respectively. This

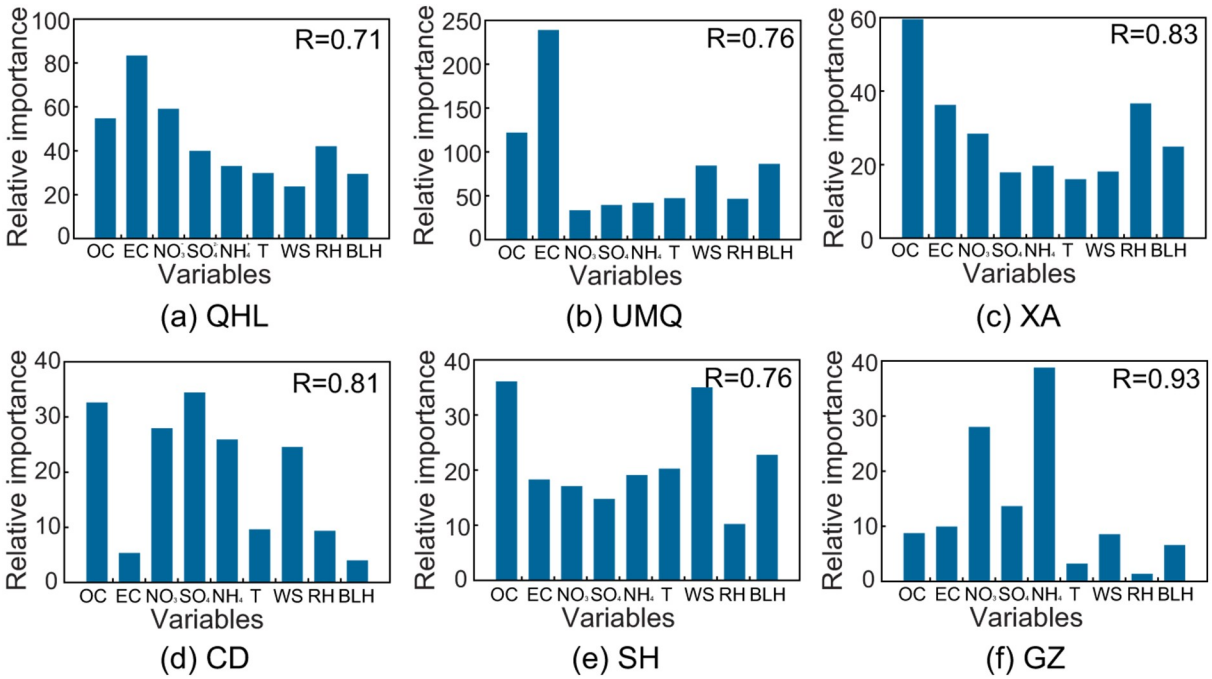

Fig. 6. Relative importance of five primary chemical constituents and four related meteorological factors contributing to the observed PM_1 mass concentration during polluted days. *R* denotes the correlation coefficient between predicted PM_1 mass concentration values and the corresponding in situ observations.

Table 5. Same as in Table 2 but for comparison of mean mass concentration ratios of PM and five major chemical compositions between PM_1 and $PM_{2.1}$.

Region	*N*	PM	EC	OM	NO_3^-	SO_4^{2-}	NH_4^+
Qinghai	53	0.71±0.10	0.84±0.16	0.79±0.10	0.71±0.12	0.80±0.10	0.94±0.09
Ürümqi	71	0.71±0.11	0.78±0.18	0.78±0.10	0.72±0.14	0.72±0.17	0.80±0.18
Xi'an	72	0.66±0.08	0.79±0.11	0.70±0.11	0.63±0.12	0.67±0.13	0.73±0.14
Chengdu	71	0.69±0.07	0.79±0.09	0.73±0.08	0.68±0.09	0.66±0.12	0.68±0.12
Shanghai	71	0.73±0.06	0.83±0.09	0.81±0.09	0.70±0.10	0.76±0.10	0.79±0.12
Guangzhou	70	0.75±0.04	0.88±0.08	0.81±0.06	0.70±0.10	0.80±0.09	0.85±0.13

implies $PM_{2.5}$ pollution in Guangzhou is mainly dominated by submicron fine particle pollution events, followed by Shanghai given the second highest ratio. On the contrary, Xi'an and Chengdu are two cities having relatively low fractions in chemical compositions. This result suggests even more diverse emission sources in these two inland cities, since a larger fraction of chemical compositions in $PM_{2.5}$ was contributed by coarser particles. Overall, our results indicate that the main sources of PM_1 and $PM_{2.5}$ in the two coastal cities were dominated by combustion processes and secondary aerosols while natural sources and mechanical emissions could contribute significantly in the two inland cities.

4. Conclusions

Based on three-year-long aerosol samplings from field campaigns, we have examined the variations of chemical components in PM_1 in six representative regions across China. The PM_1 mass concentration and its chemical constituents were compared with respect to pollution levels, seasons, and meteorological conditions. The results revealed that both PM_1 and its chemical constituents varied significantly in space and time, with high PM_1 loading observed mainly in the winter and low values in the summer. Meanwhile, a substantial increase in OM and SNA was oftentimes observed in elevating PM_1 mass concentration, particularly OM during wintertime. Compared to other species, OM had a larger overall abundance in PM_1, indicative of a more important role of primary emission and the formation of secondary aerosols in exacerbating PM_1 pollution levels during wintertime.

Comparisons of OC/EC and NO_3^-/SO_4^{2-} ratios across regions revealed that PM_1 loading in Guangzhou tended to be modulated largely by primary emissions given lower ratios of both factors throughout the year. The largest ratios of both factors in Xi'an were observed mainly in the winter, with the lowest observed in the summer. This effect could be associated with the seasonality of both emission intensity and meteorological conditions. Moreover, elevated concentrations of SNA and OM were oftentimes observed during polluted days, particularly nitrate and sulfate, though their increments differed greatly across the regions. This implies important roles of both primary emission and secondary particle formation in producing haze events. In spite of a small magnitude, a ubiquitous increase in ammonium was observed in the five major cities during wintertime, and this was found to play the most important role in modulating the variability of PM_1 mass concentration in Guangzhou.

Meteorological factors were shown to play important roles in modulating the variability of PM_1 mass loading. Our modeling practices have clearly revealed that ambient PM_1 mass concentration was largely regulated by primary emissions (e.g., Qinghai and Ürümqi) and secondary aerosol formations (e.g., Xi'an, Shanghai, and Chengdu). Meanwhile, the importance of meteorological factors was found to vary across regions under different pollution regimes. Overall, the results in this study clearly indicate that there is no common driving mechanism for haze events due to diverse sources and influential factors. Due to the data issue, an elemental analysis was not performed in the current study, but this should be included in future field campaigns to more fully investigate the driving factors behind haze events.

Acknowledgements. We are grateful to three anonymous reviewers and editors for their copious and constructive comments and suggestions. This work was financially supported by National Key R&D Plan (Grant No. 2017YFC0210000), National Natural Science Foundation of China (Grant No. 41701413), National Key R&D Plan (Grant No. 2017YFC0212703) and Strategic Priority Research Program of the Chinese Academy of Sciences (Grant No. XDB05020401). Meteorological data were acquired from the Meteorological Information Comprehensive Analysis and Process System (air temperature, relative humidity, and wind speed), and ERA-Interim reanalysis (boundary layer height) that was provided by the European Centre for Medium-Range Weather Forecasts.

REFERENCES

Altmann, A., L. Toloşi, O. Sander, and T. Lengauer, 2010: Permutation importance: A corrected feature importance measure. *Bioinformatics*, **26**, 1340–1347, https://doi.org/10.1093/bioinformatics/btq134.

An, Z. S., and Coauthors, 2019: Severe haze in northern China: A synergy of anthropogenic emissions and atmospheric processes. *Proceedings of the National Academy of Sciences of the United States of America*, **116**, 8657–8666, https://doi.org/10.1073/pnas.1900125116.

Appel, B. R., Y. Tokiwa, J. Hsu, E. L. Kothny, and E. Hahn, 1985: Visibility as related to atmospheric aerosol constituents. *Atmos. Environ.*, **19**, 1525–1534, https://doi.org/10.1016/0004-6981(85)90290-2.

Arimoto, R., and Coauthors, 1996: Relationships among aerosol constituents from Asia and the North Pacific during PEM-West A. *J. Geophys. Res.*, **101**, 2011–2023, https://doi.org/10.1029/95JD01071.

Bae, M. S., K. L. Demerjian, and J. J. Schwab, 2006: Seasonal estimation of organic mass to organic carbon in $PM_{2.5}$ at rural and urban locations in New York state. *Atmos. Environ.*, **40**, 7467–7479, https://doi.org/10.1016/j.atmosenv.2006.07.008.

Bai, K. X., N.-B. Chang, J. Y. Zhou, W. Gao, and J. P. Guo, 2019a: Diagnosing atmospheric stability effects on the modeling accuracy of $PM_{2.5}$/AOD relationship in eastern China using radiosonde data. *Environmental Pollution*, **251**, 380–389, https://doi.org/10.1016/j.envpol.2019.04.104.

Bai, K. X., K. Li, N.-B. Chang, and W. Gao, 2019b: Advancing the prediction accuracy of satellite-based $PM_{2.5}$ concentration mapping: A perspective of data mining through in situ $PM_{2.5}$ measurements. *Environmental Pollution*, **254**, 113047, https://doi.org/10.1016/j.envpol.2019.113047.

Burnett, R., and Coauthors, 2018: Global estimates of mortality associated with long-term exposure to outdoor fine particulate matter. *Proceedings of the National Academy of Sciences of the United States of America*, **115**, 9592–9597, https://doi.org/10.1073/pnas.1803222115.

Charlson, R. J., 1969: Atmospheric visibility related to aerosol mass concentration: Review. *Environ. Sci. Technol.*, **3**, 913–918, https://doi.org/10.1021/es60033a002.

Chen, G. B., and Coauthors, 2018: Spatiotemporal variation of PM_1 pollution in China. *Atmos. Environ.*, **178**, 198–205, https://doi.org/10.1016/j.atmosenv.2018.01.053.

Chow, J. C., J. G. Watson, L. W. A. Chen, W. P. Arnott, H. Moosmüller, and K. Fung, 2004: Equivalence of elemental carbon by thermal/optical reflectance and transmittance with different temperature protocols. *Environ. Sci. Technol.*, **38**, 4414–4422, https://doi.org/10.1021/es034936u.

Chow, J. C., J. G. Watson, D. H. Lowenthal, and K. L. Magliano, 2005: 2005: Loss of $PM_{2.5}$ nitrate from filter samples in central California. *Journal of the Air & Waste Management Association*, **55**, 1158–1168, https://doi.org/10.1080/10473289.2005.10464704.

Chow, J. C., J. G. Watson, L. W. A. Chen, M. C. O. Chang, N. F. Robinson, D. Trimble, and S. Kohl, 2007: The IMPROVE_A temperature protocol for thermal/optical carbon analysis: Maintaining consistency with a long-term database. *Journal of the Air & Waste Management Association*, **57**, 1014–1023, https://doi.org/10.3155/1047-3289.57.9.1014.

Dang, R. J., and H. Liao, 2019: Severe winter haze days in the Beijing–Tianjin–Hebei region from 1985 to 2017 and the roles of anthropogenic emissions and meteorology. *Atmospheric Chemistry and Physics*, **19**, 10 801–10 816, https://doi.org/10.5194/acp-19-10801-2019.

Ebenstein, A., M. Y. Fan, M. Greenstone, G. J. He, and M. G. Zhou, 2017: New evidence on the impact of sustained exposure to air pollution on life expectancy from China's Huai River Policy. *Proceedings of the National Academy of Sciences of the United States of America*, **114**, 10 384–10 389, https://doi.org/10.1073/pnas.1616784114.

Gomišček., 2004: Spatial and temporal variations of PM_1, $PM_{2.5}$, PM_{10} and particle number concentration during the AUPHEP—project. *Atmos. Environ.*, **38**, 3917–3934, https://doi.org/10.1016/j.atmosenv.2004.03.056.

Guo, J. P., and Coauthors, 2017: Declining frequency of summertime local-scale precipitation over eastern China from 1970 to 2010 and its potential link to aerosols. *Geophys. Res. Lett.*, **44**, 5700–5708, https://doi.org/10.1002/2017GL073533.

Guo, J. P., and Coauthors, 2019: Shift in the temporal trend of boundary layer height in China using long-term (1979–2016) radiosonde data. *Geophys. Res. Lett.*, **46**, 6080–6089, https://doi.org/10.1029/2019GL082666.

Guo, S., and Coauthors, 2014: Elucidating severe urban haze formation in China. *Proceedings of the National Academy of Sciences of the United States of America*, **111**, 17 373–17 378, https://doi.org/10.1073/pnas.1419604111.

Ho, T. K., 1998: The random subspace method for constructing decision forests. *IEEE Transactions on Pattern Analysis and Machine Intelligence*, **20**, 832–844, https://doi.org/10.1109/34.709601.

Holben, B. N., and Coauthors, 1998: AERONET—A federated instrument network and data archive for aerosol characterization. *Remote Sensing of Environment*, **66**, 1–16, https://doi.org/10.1016/S0034-4257(98)00031-5.

Hu, D. W., J. M. Chen, X. N. Ye, L. Li, and X. Yang, 2011: Hygroscopicity and evaporation of ammonium chloride and ammonium nitrate: Relative humidity and size effects on the growth factor. *Atmos. Environ.*, **45**, 2349–2355, https://doi.org/10.1016/j.atmosenv.2011.02.024.

Huang, R.-J., and Coauthors, 2014: High secondary aerosol contribution to particulate pollution during haze events in China. *Nature*, **514**, 218–222, https://doi.org/10.1038/nature13774.

Huang, X., and Coauthors, 2020: Enhanced secondary pollution offset reduction of primary emissions during COVID-19 lockdown in China. *National Science Review*, https://doi.org/10.1093/nsr/nwaa137.

Khan, J. Z., L. Sun, Y. Z. Tian, G. L. Shi, and Y. C. Feng, 2021: Chemical characterization and source apportionment of PM_1 and $PM_{2.5}$ in Tianjin, China: Impacts of biomass burning and primary biogenic sources. *Journal of Environmental Sciences*, **99**, 196–209, https://doi.org/10.1016/j.jes.2020.06.027.

Li, J., and Coauthors, 2014: Comparison of abundances, compositions and sources of elements, inorganic ions and organic compounds in atmospheric aerosols from Xi'an and New Delhi, two megacities in China and India. *Sci. Total Environ.*, **476-477**, 485–495, https://doi.org/10.1016/j.scitotenv.2014.01.011.

Li, Z. Q., and Coauthors, 2017: Aerosol and boundary-layer interactions and impact on air quality. *National Science Review*, **4**, 810–833, https://doi.org/10.1093/nsr/nwx117.

Li, Z. Q., and Coauthors, 2019: East Asian study of tropospheric aerosols and their impact on regional clouds, precipitation, and climate (EAST-AIR_{CPC}). *J. Geophys. Res.*, **124**, 13 026–13 054, https://doi.org/10.1029/2019JD030758.

Liu, H. J., and Coauthors, 2014: Aerosol hygroscopicity derived from size-segregated chemical composition and its parameterization in the North China Plain. *Atmospheric Chemistry and Physics*, **14**, 2525–2539, https://doi.org/10.5194/acp-14-2525-2014.

Liu, L., J. Guo, Y. C. Miao, L. Liu, J. Li, D. D. Chen, J. He, and C. G. Cui, 2018: Elucidating the relationship between aerosol concentration and summertime boundary layer structure in central China. *Environmental Pollution*, **241**, 646–653, https://doi.org/10.1016/j.envpol.2018.06.008.

Lou, M. Y., and Coauthors, 2019: On the relationship between aerosol and boundary layer height in Summer in China under different thermodynamic conditions. *Earth and Space Science*, **6**, 887–901, https://doi.org/10.1029/2019EA000620.

Miao, Y. C., S. H. Liu, J. P. Guo, S. X. Huang, Y. Yan, and M. Y. Lou, 2018: Unraveling the relationships between boundary layer height and $PM_{2.5}$ pollution in China based on four-year radiosonde measurements. *Environmental Pollution*, **243**, 1186–1195, https://doi.org/10.1016/j.envpol.2018.09.070.

Pósfai, M., and P. R. Buseck, 2010: Nature and climate effects of individual tropospheric aerosol particles. *Annual Review of Earth and Planetary Sciences*, **38**, 17–43, https://doi.org/10.1146/annurev.earth.031208.100032.

Qiao, T., M. F. Zhao, G. L. Xiu, and J. Z. Yu, 2016: Simultaneous monitoring and compositions analysis of PM_1 and $PM_{2.5}$ in Shanghai: Implications for characterization of haze pollution and source apportionment. *Science of the Total Environment*, **557–558**, 386–394, https://doi.org/10.1016/j.scitotenv.2016.03.095.

Qin, Y. M., and Coauthors, 2017: Impacts of traffic emissions on atmospheric particulate nitrate and organics at a downwind site on the periphery of Guangzhou, China. *Atmospheric Chemistry and Physics*, **17**, 10 245–10 258, https://doi.org/10.5194/acp-17-10245-2017.

Ren, Y. Q., and Coauthors, 2018: Seasonal variation and size distribution of biogenic secondary organic aerosols at urban and continental background sites of China. *Journal of Environmental Sciences*, **71**, 32–44, https://doi.org/10.1016/j.jes.2017.11.016.

Shao, P. Y., and Coauthors, 2018: Characterizing remarkable changes of severe haze events and chemical compositions in multi-size airborne particles (PM_1, $PM_{2.5}$ and PM_{10}) from January 2013 to 2016–2017 winter in Beijing, China. *Atmos. Environ.*, **189**, 133–144, https://doi.org/10.1016/j.atmosenv.2018.06.038.

Shi, Y., J. M. Chen, D. W. Hu, L. Wang, X. Yang, and X. M. Wang, 2014: Airborne submicron particulate (PM_1) pollution in Shanghai, China: Chemical variability, formation/dissociation of associated semi-volatile components and the impacts on visibility. *Science of the Total Environment*, **473–474**, 199–206, https://doi.org/10.1016/j.scitotenv.2013.12.024.

Sun, Y. L., and Coauthors, 2020: Chemical differences between PM_1 and $PM_{2.5}$ in highly polluted environment and implications in air pollution studies. *Geophys. Res. Lett.*, **47**, e2019GL086288, https://doi.org/10.1029/2019GL086288.

Turpin, B. J., and H. J. Lim, 2001: Species contributions to $PM_{2.5}$ mass concentrations: Revisiting common assumptions for estimating organic mass. *Aerosol Science and Technology*, **35**, 602–610, https://doi.org/10.1080/02786820119445.

Wang, G. H., and Coauthors, 2014: Evolution of aerosol chemistry in Xi'an, inland China, during the dust storm period of 2013—Part 1: Sources, chemical forms and formation mechanisms of nitrate and sulfate. *Atmospheric Chemistry and Physics*, **14**, 11 571–11 585, https://doi.org/10.5194/acp-14-11571-2014.

Wang, G. H., and Coauthors, 2016: Persistent sulfate formation from London Fog to Chinese haze. *Proceedings of the National Academy of Sciences of the United States of America*, **113**, 13 630–13 635, https://doi.org/10.1073/pnas.1616540113.

Wang, G. H., and Coauthors, 2018: Particle acidity and sulfate production during severe haze events in China cannot be reliably inferred by assuming a mixture of inorganic salts. *Atmospheric Chemistry and Physics*, **18**, 10 123–101 32, https://doi.org/10.5194/acp-18-10123-2018.

Wang, J. F., and Coauthors, 2020: Fast sulfate formation from oxidation of SO_2 by NO_2 and HONO observed in Beijing haze. *Nature Communications*, **11**, 2844, https://doi.org/10.1038/s41467-020-16683-x.

Wang, Y. Y., and Coauthors, 2019: Distinct ultrafine- and accumulation - mode particle properties in clean and polluted urban environments. *Geophys. Res. Lett.*, **46**, 10 918–10 925, https://doi.org/10.1029/2019GL084047.

Wang, Z. B., and Coauthors, 2017: New particle formation in China: Current knowledge and further directions. *Science of the Total Environment*, **577**, 258–266, https://doi.org/10.1016/j.scitotenv.2016.10.177.

WMO, 2001: Strategy for the implementation of the global atmosphere watch programme (2001–2007). GAW Rep. No. 142, WMO TD No. 1077.

Wu, C., and Coauthors, 2020: The characteristics of atmospheric brown carbon in Xi'an, Inland China: Sources, size distributions and optical properties. *Atmospheric Chemistry and Physics*, **20**, 2017–2030, https://doi.org/10.5194/acp-20-2017-2020.

Xin, J. Y., and Coauthors, 2015: The campaign on atmospheric aerosol research network of China: CARE-China. *Bull. Amer. Meteor. Soc.*, **96**, 1137–1155, https://doi.org/10.1175/BAMS-D-14-00039.1.

Yang, F., and Coauthors, 2011: Characteristics of $PM_{2.5}$ speciation in representative megacities and across China. *Atmospheric Chemistry and Physics*, **11**, 5207–5219, https://doi.org/10.5194/acp-11-5207-2011.

Yao, L., and Coauthors, 2018: Atmospheric new particle formation from sulfuric acid and amines in a Chinese megacity. *Science*, **361**, 278–281, https://doi.org/10.1126/science.aao4839.

Yao, X. H., C. K. Chan, M. Fang, S. Cadle, T. Chan, P. Mulawa, K. B. He, and B. M. Ye, 2002: The water-soluble ionic composition of $PM_{2.5}$ in Shanghai and Beijing, China. *Atmos. Environ.*, **36**, 4223–4234, https://doi.org/10.1016/S1352-2310(02)00342-4.

Yue, H. B., C. Y. He, Q. X. Huang, D. Yin, and B. A. Bryan, 2020: Stronger policy required to substantially reduce deaths from $PM_{2.5}$ pollution in China. *Nature Communications*, **11**, 1462, https://doi.org/10.1038/s41467-020-15319-4.

Zamora, M. L., and Coauthors, 2019: Wintertime aerosol properties in Beijing. *Atmospheric Chemistry and Physics*, **19**, 14 329–14 338, https://doi.org/10.5194/acp-19-14329-2019.

Zhang, X. Y., 2014: Characteristics of the chemical components of aerosol particles in the various regions over China. *Acta Meteorologica Sinica*, **72**, 1108–1117, https://doi.org/10.11676/qxxb2014.092. (in Chinese with English abstract)

Zhang, Y. J., and Coauthors, 2018: Evidence of major secondary organic aerosol contribution to lensing effect black carbon absorption enhancement. *npj Climate and Atmospheric Science*, **1**, 47, https://doi.org/10.1038/s41612-018-0056-2.

Zhao, F. C., and Coauthors, 2020: Aerosol characteristics and impacts on weather and climate over the Tibetan Plateau. *National Science Review*, **7**, 492–495, https://doi.org/10.1093/nsr/nwz184.

Zheng, C. W., and Coauthors, 2017: Analysis of influential factors for the relationship between $PM_{2.5}$ and AOD in Beijing. *Atmospheric Chemistry and Physics*, **17**, 13 473–13 489, https://doi.org/10.5194/acp-17-13473-2017.

Zhu, X. W., and Coauthors, 2018: Mixing layer height on the North China Plain and meteorological evidence of serious air pollution in southern Hebei. *Atmospheric Chemistry and Physics*, **18**, 4897–4910, https://doi.org/10.5194/acp-18-4897-2018.

Zou, B., J. W. You, Y. Lin, X. L. Duan, X. G. Zhao, X. Fang, M. J. Campen, and S. X. Li, 2019: Air pollution intervention and life-saving effect in China. *Environment International*, **125**, 529–541, https://doi.org/10.1016/j.envint.2018.10.045.